Phase-Encoded Retinotopic Mapping in Humans with DOT

Brian R. White[1], Benjamin W. Zeff[2], Bradley L. Schlaggar[2], Hamid Dehghani[3], Joseph P. Culver[2]
[1]*Department of Physics and School of Medicine, Washington University, St. Louis, MO 63110*
[2]*Department of Radiology, Washington University School of Medicine, St. Louis, MO 63110*
[3]*School of Physics, University of Exeter, Exeter, UK*
E-mail: culverj@mir.wustl.edu, Tel: (314)-747-1341, Fax: (314)-747-5191

Abstract: We have developed a high-density neuroimaging DOT system with improved depth discrimination and lateral resolution. The advantages are demonstrated through cortical maps of phase-encoded traveling waves in the full visual field of adult humans.

OCIS Codes: (170.2655) Functional monitoring and imaging; (170.3880) Medical and biological imaging; (110.3080) Infrared Imaging; (170.0110) Imaging systems

1. Introduction

The advent of functional neuroimaging has dramatically changed the field of neuroscience research. This revolution has primarily been driven by functional magnetic resonance imaging (fMRI) using a blood oxygen level dependent (BOLD) contrast. However, BOLD-fMRI, with a single hemodynamic contrast and a large scanner geometry has limitations in the study of neonates and those with brain injury, and it is often not applicable for clinical evaluation of small children and critically ill patients. Near-infrared spectroscopy (NIRS) neuroimaging techniques can potentially address these limitations of fMRI. Portable NIRS instrumentation and wearable imaging caps can be used to measure both oxy- and deoxyhemoglobin, allowing bedside imaging with a more complete picture of brain hemodynamics. However, NIRS has been limited by low depth penetration, poor lateral resolution, and difficulty in separating superficial and neuronal signals. For example, in the visual cortex, NIRS studies have previously been limited to only detecting contralateral activations [1,2]. Diffuse optical tomography (DOT) methods can improve upon NIRS performance through the use of overlapping measurements. This method dramatically increases lateral resolution and improves the ability to separate superficial signals from true brain activations. However severe attenuation of light in the brain due to high blood volume creates challenges for DOT instrumentation. We have recently developed a DOT system that has high dynamic range and low crosstalk such that it can support high-density imaging arrays for brain imaging [3]. Here, we report the use of this system to perform retinotopic mapping of the adult human visual cortex. The visual cortex is an ideal benchmark for functional neuroimaging techniques due to its detailed structure. Every area of the visual field maps to different areas of the cortex; these maps can thus be used to evaluate the resolution performance of neuroimaging systems in vivo. We used phase-encoded stimuli, which sequentially excite the entire retina in a periodic manner, generating traveling waves of neuronal activity in the visual cortex. This allows us to map the pattern of polar angle and eccentricity with higher resolution than that previously obtained with optical imaging.

2. Methods

All scans were conducted with our custom-built continuous wave high-density DOT imaging system [3]. Briefly, the imaging cap consists of 24 source positions (LEDs with two near-infrared wavelengths—750 nm and 850 nm—at each position) and 28 APD detectors interleaved in a high-density array (Figure 1*a*). First- (13 mm), through fourth-nearest-neighbor (48 mm) optode pairs are well above the noise floor, a total of 348 measurements at a frame rate of greater than 10 Hz.

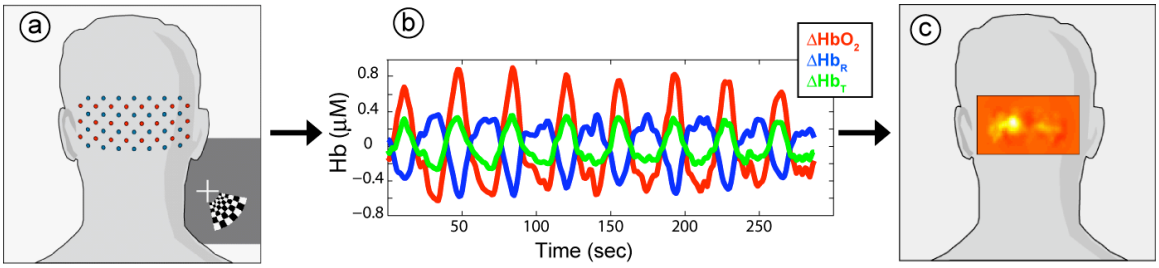

Fig. 1. The high-density DOT imaging system. **(a)** A schematic showing the placement of the imaging grid (sources in red, detectors in blue) over the occipital cortex, with an inset example of a visual stimulus. **(b)** Time trace of a 6 x 6 mm region within the left visual cortex from one subject showing the periodic activation through eight cycles of the counter-clockwise

wedge stimulus. High contrast-to-noise is seen in all three hemodynamic constrasts (oxyhemoglobin in red, deoxyhemoglobin in blue, and total hemoglobin in green). **(c)** One image frame from a scanning session, due to the stimulus shown in (a) (change in [ΔHbT] is shown with orange being no change in concentration, white an increase, and black a decrease).

Subjects were recruited from the Washington University School of Medicine community, and written informed consent was obtained. Subjects were seated facing an adjustable screen, and the imaging pad was attached over the occipital cortex with Velcro. Visual stimuli all consisted of reversing (10 Hz) logarithmic checkerboards on a 50% gray background. Counter-clockwise and clockwise rotating wedges (inner radius 1.5º, outer radius 10.5º, width 60º, rotation 10º/sec) mapped polar angle within the visual field. Expanding and contracting rings (minimum radius 1.5º, maximum radius 10º, width 3 rings, 18 positions with 2 sec per position) mapped eccentricity. This follows well-established fMRI paradigms [4-6]. Each stimulus lasted for 8 cycles, for about 21 min total scanning time.

Optode-pair data was filtered to remove long-term trends and high-frequency noise. Then, all first-nearest neighbors were averaged, and this global superficial signal was then removed by linear regression from all channels (similar to the method of [7]). Then, a second low-pass filter removed the pulse. The resulting signals were resampled to 1 Hz and imaged using an A-matrix derived from finite-element modeling of a two-layer hemispherical head model. Images are presented as posterior coronal projection of a cortical shell through the three-dimensional images. (For further details on the processing methods, see *Zeff et al.* [3].) Fourier analysis can then be conducted; for every pixel, finding the phase at the stimulus frequency (1/36 Hz), allows us to determine the correspondence between that point in the cortex and the visual field [5,6,8].

3. Results

The high-density DOT data provides clear detection of functional activations with high contrast-to-noise (Figure 1*b*,*c*). In axial slices, activations are localized at depth with little change in hemoglobin present in the outer layer. The measured hemoglobin timecourses are in good agreement with previous fMRI and NIRS studies of neurovascular coupling. The lateral resolution of the system is highlighted in Figure 2, where activations above FWHM from single runs in individual subjects are shown for both polar angle and eccentricity.

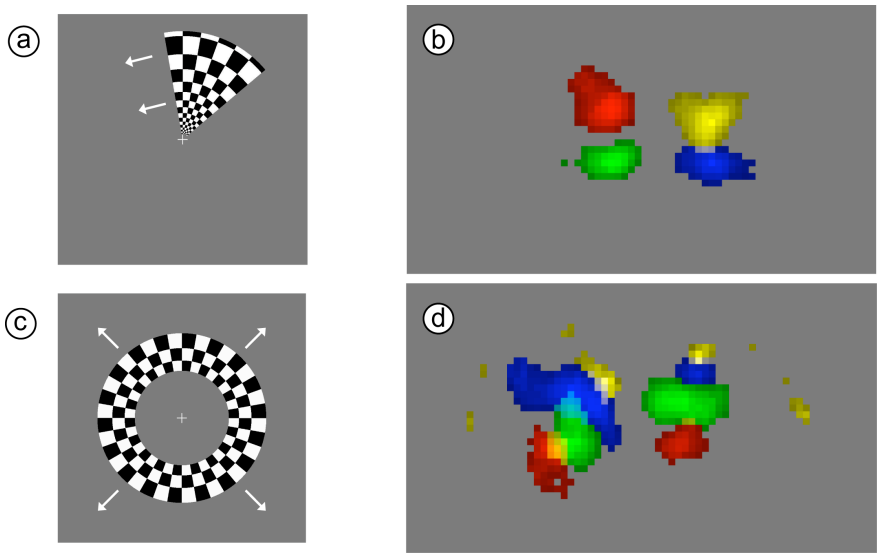

Fig. 2. (a) Still frame from wedge stimulus showing counter-clockwise direction of motion. **(b)** Four ΔHbT activation images (shown above FWHM) from counter-clockwise sweep (Yellow: timepoint 3, Red: timepoint 12, Green: timepoint 21, Blue: timepoint 30). **(c)** Still frame from ring stimulus showing expanding direction of motion. **(d)** Four ΔHbT activation images (shown above FWHM) from expanding ring (same timepoint coloring).

Figure 3 shows results of using the phase-encoded activations to determine retinotopic maps. Converting to phase images through Fourier analysis allows every cortical pixel to be assigned a corresponding point in the visual field (e.g., Figure 3*c*). We are in the process of performing the same protocol in fMRI to compare the results of the two neuroimaging methods. Figure 3*d* shows the results of having the same subject view the same stimulus in an fMRI. A coronal slice was then taken through primary visual cortex. Phase analysis performed in an identical manner shows a similar retinotopic pattern to than obtained with DOT (compare Figure 3*c* and 3*d*).

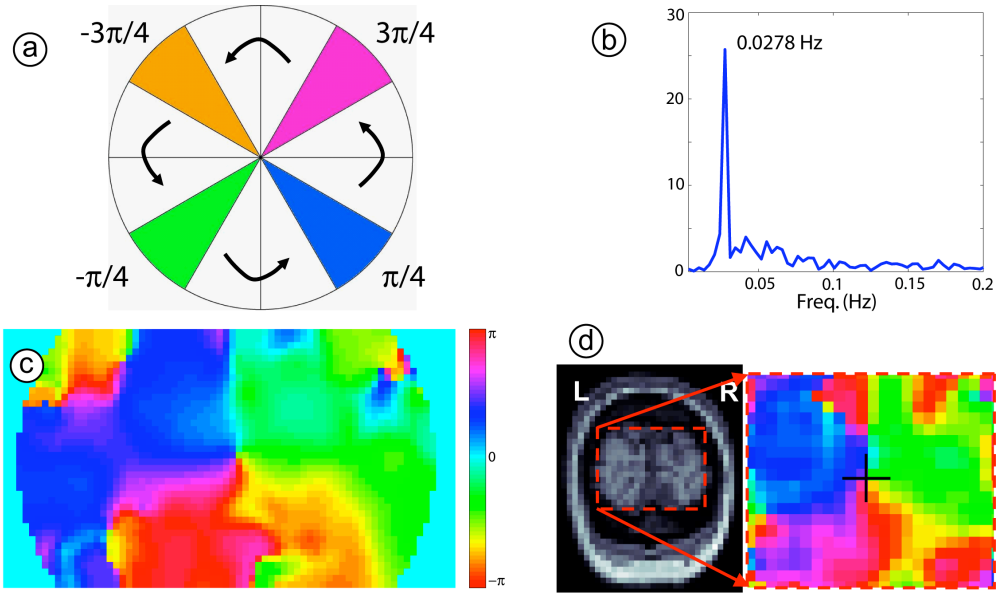

Fig. 3. Data processing of retinotopy data (ΔHbT). **(a)** Convention for defining phase of the sweep stimulus. **(b)** The Fourier transform of the time trace from a single pixel (counter-clockwise sweep) highlights the high SNR of the response at the frequency of the rotating stimulus (1/36 Hz). **(c)** Phase map showing relationship between cortical location and the visual field. Comparison with (a) shows that visual stimuli map most strongly into the opposite visual cortex, with additional structure in the periphery. **(d)** The same protocol performed in fMRI. An anatomical slice through primary visual cortex is shown. The BOLD data from this slice was analyzed using the above methods. The similarity with (c) validates the retinotopic results found with DOT.

4. Conclusions

These results demonstrate how our high-density DOT neuroimaging system is able to map the visual cortex with remarkable resolution from single data runs in individual subjects. To our knowledge, this is the first use of DOT to move beyond activation images to provide higher-order information such as cortical maps. We are in the process of directly comparing the results of DOT retinotopic imaging with those of fMRI. As these methods establish the validity of DOT against standard neuroimaging benchmarks, we have a stronger foundation for applying DOT to analyzing cortical function in our target populations, such as children and neonates. We believe that these results are an important step towards DOT fulfilling its promise for neuroimaging and that the resolution highlighted here will allow us to tackle many other interesting neuroscience questions in areas previously inaccessible to either fMRI or optical imaging.

[1] V.Y. Toronov, X. Zhang, and A.G. Webb, "A spatial and temporal comparison of hemodynamic signals measured using optical and functional magnetic resonance imaging during activation in the human primary visual cortex," NeuroImage **34**, 1136-1148 (2007).

[2] W.N.J.M. Colier, V. Quaresima, R. Wenzel, M.C. van der Sluijs, B. Oeseburg, M. Ferrari, and A. Villringer, "Simultaneous near-infrared spectroscopy monitoring of left and right occipital areas reveals contra-lateral hemodynamic changes upon hemi-field paradigm," Vis. Res. **41**, 97-102 (2001).

[3] B.W. Zeff, B.R. White, H. Dehghani, B.L. Schlaggar, and J.P. Culver, "Retinotopic mapping of adult human visual cortex with high-density diffuse optical tomography," PNAS **104**, 12169-12174 (2007).

[4] S.A. Engel, D.E. Rumelhart, B.A. Wandell, A.T. lee, G.H. Glover, E-J. Chichilnisky, and M.N. Shadlen, "fMRI of human visual cortex," Nature **369**, 525 (1994).

[5] S.A. Engel, G.H. Glover, and B.A. Wandell, "Retinotopic organization in human visual cortex and the spatial precision of functional MRI," Cereb. Cortex **7**, 181-192 (1997).

[6] J. Warnking, M. Dojat, A. Guérin-Dugué, C. Delon-Martin, S. Olympieff, N. Richard, A. Chéhikian, and C. Segebarth, "fMRI retinotopic mapping—step by step," NeuroImage **17**, 1665-1683 (2002).

[7] R.B. Saager and A.J. Berger, "Direct characterization and removal of interfering absorption trends in two-layer turbid media," J. Opt. Soc. Am. A **22**, 1874-1882 (2005).

[8] M.I. Sereno, A.M. Dale, J.B. Reppas, K.K. Kwong, J.W. Belliveau, T.J. Brady, B.R. Rosen, and R.B.H. Tootell, "Borders of multiple visual areas in humans revealed by functional magnetic resonance imaging," Science **268**, 89-893 (1995).